Journal of Alloys and Compounds xxx (2008) xxx–xxx

Contents lists available at ScienceDirect

Journal of Alloys and Compounds

journal homepage: www.elsevier.com/locate/jallcom

The dynamic nature of hydrogen in the α and β phases in the Gd(0 0 0 1)/W(1 1 0) system: STM observations

H. Realpe[a,c,*], N. Shamir[b], Y. Manassen[a], M.H. Mintz[b,c]

[a] Department of Physics and the Ilse Katz Center of Science and Technology in the nm scale, Ben Gurion University of the Negev, P.O. Box 653, Beer Sheva 84105, Israel
[b] Nuclear Research Center-Negev, P.O. Box 9001, Beer Sheva 84190, Israel
[c] Department of Nuclear Engineering, Ben Gurion University of the Negev, P.O. Box 653, Beer Sheva 84105, Israel

ARTICLE INFO

Article history:
Received 30 April 2008
Received in revised form 4 June 2008
Accepted 5 June 2008
Available online xxx

Keywords:
Scanning tunneling microscopy
Diffusion and migration
Nucleation
Surface stress
Lanthanides
Hydrides

ABSTRACT

Scanning tunneling microscopy was utilized to follow the effects of low dose exposures of hydrogen on Gd(0 0 0 1) islands grown on a W(1 1 0) substrate. Two types of time fluctuating effects were observed. First, periodic appearance–disappearance of some of the Gd islands, which was attributed to concentration fluctuations of H dissolved in the α-phase. Second, the development of hydride β-phase nuclei displayed irregular growth–shrinkage behavior, concurrent with irregular morphological variations. This behavior was also attributed to H concentration time-variations induced by the strain field that accompanies the hydride growth. It seems thus that both, the H dissolution in the α-phase, and the precipitation of the hydrides (β-phase) within the α-phase, display irregular "wave" like behavior in this system.

1. Introduction

Nucleation and growth of hydrides on the surface of hydride-forming metals and alloys characterize the very initial stages of the massive hydrogen reactions. The understanding of the mechanism involved in these stages is important both from the fundamental as well as from the practical points of view (e.g. in preventing hydrogen corrosion, in designing kinetic experiments, in nuclear reactor safety, etc.).

These nucleation and growth processes are quite complex due to the very heterogeneous characteristics of such "real life" systems, i.e. polycrystallinity, oxide coatings, etc. In fact, different "families" of hydride precipitates were identified and qualitatively attributed to different types of defects present at the metal–oxide interfaces or at the oxide layers coating the metal surfaces [1–3]. Direct observations of the very initial development stages of such hydrides on well-defined single crystal surfaces may substantiate some of the qualitative hypotheses made for the "real life" samples, and may provide additional understanding of these complex mechanisms. A pioneering attempt in this direction has been made by utilizing STM observations on Gd(0 0 0 1) islands grown on a W(1 1 0) substrate [4–7]. Low dose hydrogen exposures (in the range of 0.1–9.0 L, 1 L = 1.33×10^{-4} Pa s) indicated that adsorption starts at crystallographic surface imperfections which form the initial nucleation centers of the hydride [4–6]. From these centers, a domain like spreading develops. These observations are consistent with the qualitative hypotheses that the very initial nucleation and growth stages of the hydrides take place preferentially at defect sites on the metal [2,3]. Still, some surprising and non-anticipated phenomena were recently observed for this system [7]. It turned out that exposing the sample to hydrogen (with doses of 1–2 L) induced the appearance of "new" Gd islands that in fact already existed before, but were "invisible" to the STM. Moreover, a time fluctuating effect of periodic appearance–disappearance of these Gd islands (in time scales of hours) was displayed. This unusual behavior was attributed to the electrical conductivity of the Gd/W interface and to periodic changes in the conductivity of these interfaces in some specific islands, due to the dissolved hydrogen [7].

In the present article a detailed discussion of the mechanism associated with such periodic changes, and their implication to the dynamics of H dissolution, is presented. Also, the time behavior of hydrides nucleation and growth has been studied and interpreted.

* Corresponding author at: Department of Nuclear Engineering, Ben Gurion University of the Negev, P.O. Box 653, Beer Sheva 84105, Israel.
E-mail address: realpe@bgu.ac.il (H. Realpe).

0925-8388/$ – see front matter © 2008 Elsevier B.V. All rights reserved.
doi:10.1016/j.jallcom.2008.06.013

2. Experimental

2.1. STM setup

A scanning probe microscopy (SPM) (Park Scientific Instruments Autoprobe VP2), including STM, contact-AFM and non-contact-AFM, was installed into a UHV surface analysis chamber (Vacuum Generators UHV Chamber). To support this chamber, a structural frame was constructed, which consists of a basis table (Workshop Construction) and four pneumatic insulating legs (Newport Stabilizer Pneumatic Isolators). The chamber was joined to a system of vacuum pumps: an ion diode pump (Varian Vacuum Plus 500 Diode Pump), and a turbo molecular pump (Pfeiffer-Balzers TPU 110) backed by a rotary vane pump.

In addition to the SPM the chamber is equipped with a Scanning Auger Microscope (SAM: PHI-545), a quadrupole gas analyzer (Varian 978-1000), an ionization gauge (Vacuum Generators Ion Gauge IGC 10), a Titanium Sublimation Pump (TSP: PHI ULTEK TSP), an electron gun evaporator (Vacuum Generator s EG2), a quartz crystal deposition monitor (Inficon XTM/2), an ion gun (PHI 5 KV Ion Gun) for sputtering, and a manipulation system that includes a X–Y–Z–θ manipulator (Modified PHI manipulator), on which a heating stage (up to 2600 K) was workshop built, which can rotate the sample between the working point of the SAM plus sputtering gun (enabling cleaning as well as depth profiles and also controlled introduction of surface damage) and the evaporation cell. The sample is moved between the SPM and manipulator by a coaxial pincer grip wobble-stick (Vacuum Generators). Gas containers, pipelines and leak-valves were installed for argon for sputtering and nitrogen to keep the vacuum system uncontaminated and clean during opening, and for hydrogen and oxygen to react with the metal surfaces under study. In line with the hydrogen feeding tube, a palladium filter was installed in order to obtain high purity gas hydrogen for the reaction experiments with gadolinium. Besides the ionization gauge two other pressure gauges were installed: a capacitance diaphragm gauge (MKS Baratron 722 A; range: 66.5–133,000 Pa) and a cold cathode gauge (MKS HPS 423 I-MAG; range: 1.33×10^{-9} to 1.33 Pa).

The entire chamber, its fittings and devices were long-term baked in order to bring UHV conditions, reaching a basis pressure of 2×10^{-8} Pa. The SPM was successfully operated in all its modes (scanning tunneling microscopy, contact and non-contact atomic force microscopy) inside the chamber.

Tungsten is a very high melting material and in order to clean it very high temperatures must be reached. A major challenge in this system was the requirement to heat the sample to 1730 K and beyond. A special heating system was constructed. The heating is though resistive heating by passing currents close to 80 A through the sample.

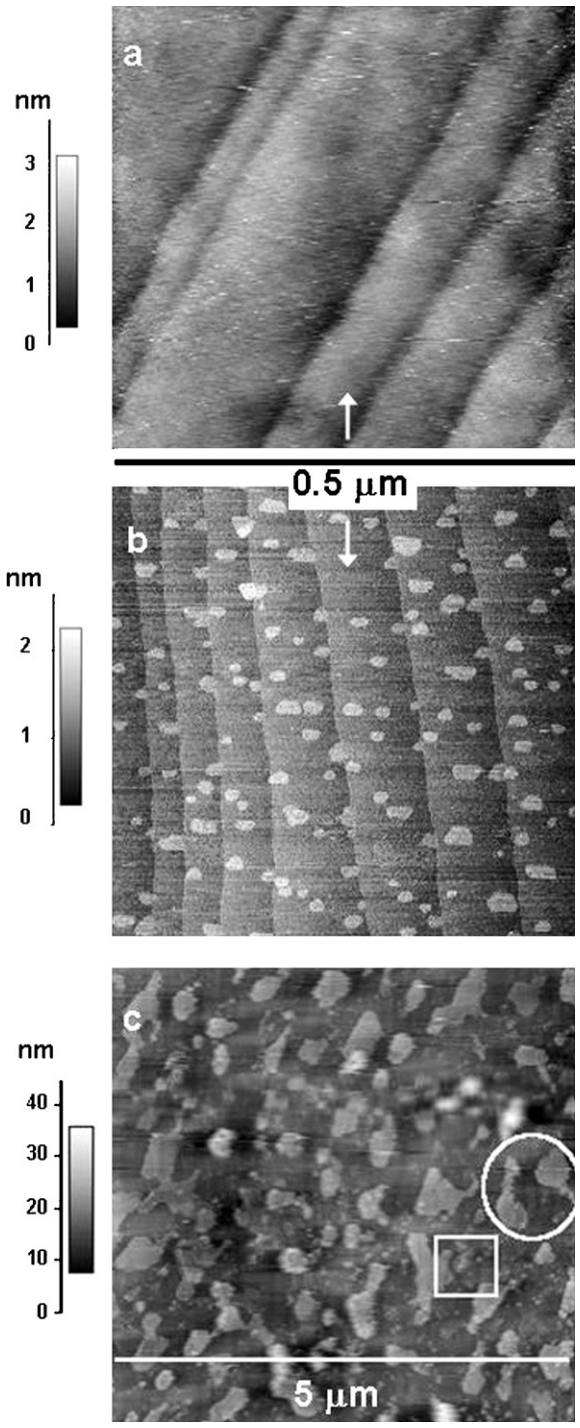

Fig. 1. STM images of (a) a clean W(1 1 0) surface served as the substrate for the growth of the Gd(0 0 0 1) islands; (b) islands pattern, observed after deposition of 2.5 ML of gadolinium and annealing at 920 K for 9 min; (c) islands pattern, observed after deposition of 14 ML of gadolinium and annealing at 920 K for 14 min (note the difference of scale, as compared to a and b).

Table 1
AES line intensities (%), obtained for the Gd(0 0 0 1)/W(1 1 0) system, for three deposition doses (see text)

Total Gd deposition dose (apparent monolayers, ML)	2.5	10.5	14
Clean W(1 1 0) surface (before deposition)			
W	96	97.6	92.8
C	3.6	1.9	6.6
O	0.4	0.5	0.6
After room temperature deposition			
W	54.5	11.6	6.6
Gd	31.3	72.9	77.1
C	11.0	9.2	8.9
O	3.2	6.3	7.4
After heat treatment (920 K/9–14 min)			
W	52.0	44.1	39.5
Gd	30.5	36.2	33.5
C	12.7	13.8	19.0
O	4.7	5.9	8.0

2.2. Sample preparation and characterization

2.2.1. Deposition patterns

A W(1 1 0) crystal served as the substrate for the growth of the Gd islands. The crystal was cleaned by repeated cycles of heating at 1760 K in oxygen and flashing up to 2600 K [8]. These cycles were repeated until the carbon AES signal, appearing at the end of the flashing stage stabilized to a relatively low value (of a few percent). The STM image of such a clean W(1 1 0) surface is presented in Fig. 1a, displaying a terrace pattern, with terrace widths in the range of 0.03–0.15 μm. The Gd films were deposited by means of an e-beam evaporator. During Gd deposition the pressure raised up to 1×10^{-7} Pa. The surface of the sample was characterized by AES and the sample was then annealed at 920 K for about 9–16 min. The sample was then cooled down to room temperature, analyzed again by AES and imaged by STM. Table 1 summarizes the AES data obtained for these sets of such preparations, one with a low deposition dose (total of about 2.5 monolayers, ML, of gadolinium) and another two with higher depositions (10–14 ML). Fig. 1b and c illustrates the islands patterns obtained for the lower and higher depositions, respectively.

It is seen (Fig. 1b) that for low deposition doses (2–3 ML), small islands (ca. of 10–30 nm lateral dimensions) are randomly formed on the W(1 1 0) surface, with no preference towards a certain location on the W(1 1 0) terraces, i.e. the islands are formed evenly at the centers or edges of terraces, or even cover the borders of between two adjacent terraces. The height distribution of these islands (analyzed by STM) ranges between about 5 and 9 Å. Assuming that the spacing between the Gd(0 0 0 1) planes is 2.89 Å, this means 2–3 ML thick islands. The total lateral cover-

Please cite this article in press as: H. Realpe, et al., J. Alloys Compd. (2008), doi:10.1016/j.jallcom.2008.06.013

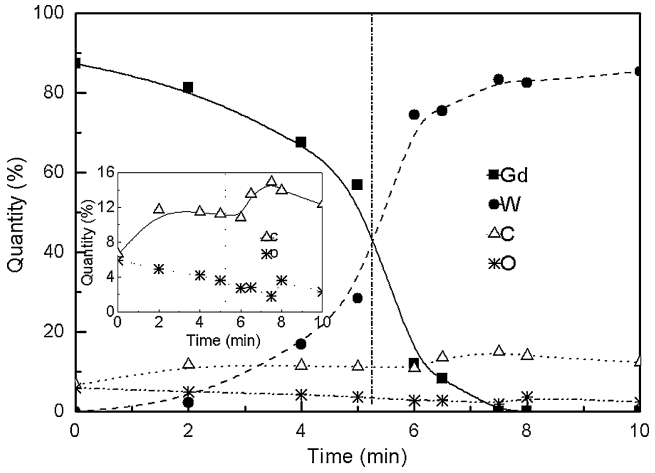

Fig. 2. AES depth profiles of: relative quantity of W, Gd, O, and C crossing the Gd/W interface (dotted line); the O and C profiles are more clearly displayed in the inset.

age of the W by the islands is relatively low, about 13% of the W surface. Hence, if the spacing between the islands was composed of the clean W substrate, the amount of Gd contained in the islands could account for only 15–16% of the total initially deposited dose (~2.5 ML, as measured by the deposition thickness monitor). It is thus concluded that a 1–2 ML of Gd is coating the spacing between the islands, i.e. a Stranski–Krastanov mode of Gd growth is taking place for this system. This conclusion is consistent with the previous STM observations reported in the literature [4,5,9]. For the higher deposition doses (Fig. 1c), the lateral size of the islands spans a relatively wide distribution, ranging between 0.05 and 0.06 μm (a large number of small islands) up to 0.4–0.7 μm (a small number of large islands). The height of these islands (determined by STM) is in the range of about 60–150 Å, i.e. 20–50 ML.

Referring to the AES data in Table 1, it is seen that the Gd/W signals intensity ratio changes during the heat treatments applied to these higher deposition doses (from values of 6–12 before treatment to values of 0.8 after heat treatments). These treatments induced the attenuation of the initial (as-deposited) Gd signal and the increase of the corresponding W signal. It seems that the ambient temperature deposition of the gadolinium lead to the formation of a continuous layer, i.e. the apparent 10–14 ML deposition dose produces a more or less smooth layer of about the same thickness (possibly with a surface roughness of the order of 1–3 ML, as explained below). However, during the following heat treatment, a Stranski–Krastanov growth of islands takes place and the continuous 10–14 ML layer converts into the pattern displayed in Fig. 1c, i.e. islands of 20–50 ML heights, connected by a 1–2 ML gadolinium film.

Quantitative calculations of the AES signal intensities, made for the two above structures confirm the respective changes in the Gd/W ratio observed in Table 1. It should be noted that unlike the above annealing-induced changes observed for the 10–14 ML depositions, no heat-induced changes were observed for the 2.5 ML deposition case (see Table 1).

It is thus likely that the kinetic limitations controlling the ambient-temperature deposition characteristics enable the development of islands formation of a very limited size (as produced for the 2.5 ML case). For the lower deposition dose, the developed room temperature pattern is close to that which is thermodynamically stable; hence no further significant changes are produced during the higher temperature treatments. However, for higher deposition doses, the lower temperatures kinetic limitations might enable the formation of a film with a certain surface roughness (of the order of 1–3 ML heights), but not allow the development of the thermodynamically stable pattern which is attained only during higher temperature treatments.

As for the depth distribution of the oxygen and carbon contaminations, Fig. 2 presents typical AES depth profiles across an as deposited Gd layer (before the annealing stage). An interesting feature that is apparent in these profiles is the appearance of oxygen and carbon contamination peaks at the Gd/W interface region. It is apparent that the locations of the carbon and oxygen peaks do not coincide, and the former is located at the Gd side of the interface, while the latter is at the W side. Anyhow, the increased contamination levels at that interface may lead to the formation of non-metallic insulating thin layers between some of the Gd islands (formed during the following annealing stage) and the W substrate. This issue will further be discussed in the interpretation of the experimental results (Section 4).

2.2.2. Hydrogen dosing

After each cycle of gadolinium evaporation – AES characterization – heat treatment—AES characterization and STM imaging of the formed island patterns, described in Section 2.2.1, ultra-high-purity (UHP) hydrogen gas was introduced to the vacuum chamber through a palladium membrane. The exposure pressure was 8.3×10^{-7} Pa, as monitored by the ion gauge (without correction), and the exposure dose, characterized in Langmuirs, was determined by the exposure time. Following a given exposure, the system was evacuated to its base pressure ($\sim 2 \times 10^{-8}$ Pa) and consecutive STM images, of the same area imagined prior to the H_2 dosing, were performed at time intervals of about 30 min.

3. Results

3.1. The α-phase region

Figs. 3 and 4 present a sequence of STM images of certain areas on the sample, displayed in Fig. 1c (labeled in Fig. 1c, by a circle and a rectangle, respectively) before hydrogen exposure (a) and after 1.5 L H_2 dosing (b–j). The time interval between two consecutive images is about 30 min. In both figures it is seen that periodic changes are induced in the STM images by hydrogen exposure, even for such a relatively low dose. It should be noted that the STM images, taken for comparative time scales (i.e. hours) without exposure to H_2 remain stable, without any noticeable changes. However, hydrogen absorption initiates periodic appearances-disappearances of some of the Gd islands. Thus, for example, it is seen in Fig. 3 that about an hour after the hydrogen exposure (Fig. 3c), a new island (labeled by arrow 1) clearly appears. It starts to fade out after about half an hour (Fig. 3d), but reappears again (Fig. 3e), and disappears again (Fig. 3f and g). Similarly, on the same imaged area a new island appears with a type of a "bridge" connecting it to an already existing island (marked by arrow 2). The new-formed "bridge", however, disappears in the next images (Fig. 3f and g), leaving the two islands "disconnected".

Another similar example of such a dynamic behavior is illustrated in Fig. 4. The appearance of a large island (with dimensions of about 0.6 μm × 0.2 μm) is evident about 1.5 h after hydrogen exposure (Fig. 4e). This island exists for about another 1.5 h (Fig. 4e–g) then starts to fade out (Fig. 4h and i) and disappears (Fig. 4j). Fig. 5 demonstrates the height profile of this periodically appearing–disappearing island, as measured at its most developed stage (Fig. 4h), along the marked line. The height scale of the island is about 40 Å, i.e. about 14 ML of gadolinium layers. This height scale corresponds to the height distribution of the gadolinium islands, formed on the surface (of Fig. 1c), prior to hydrogen exposure. Hence, the periodically appearing–disappearing islands are of about the same dimensions (both lateral and height) as the "normal" islands, observed after the deposition and annealing procedure.

As will be discussed in Section 4, the above effects seem to be associated with periodic changes in the local concentration of hydrogen that is dissolved in the gadolinium islands (i.e. the α-phase region), and not to a real assembling–disassembling of islands.

3.2. The β-phase hydride

Besides the α-phase hydrogen-induced effects there are additional changes, possibly related to the hydride (i.e. the β-phase) nucleation. This is manifested by the appearance of small spots (ca. 100–500 Å) on top of the islands, as demonstrated in Fig. 6.

In conventional nucleation and growth theory, the precipitated product nuclei start a spontaneous growth process after reaching a certain critical size where the energy gain, obtained by the bulk reaction free energy overcomes the energy loss resulted by the formation of a product–reactant interface. In order to follow the nucleation and growth kinetics of the above hydride precipitates, as a function of the precipitates size, a two-step hydrogen exposure experiment has been performed (on a surface with an initial islands pattern similar to that of Fig. 1c). In the first stage, the sam-

Please cite this article in press as: H. Realpe, et al., J. Alloys Compd. (2008), doi:10.1016/j.jallcom.2008.06.013

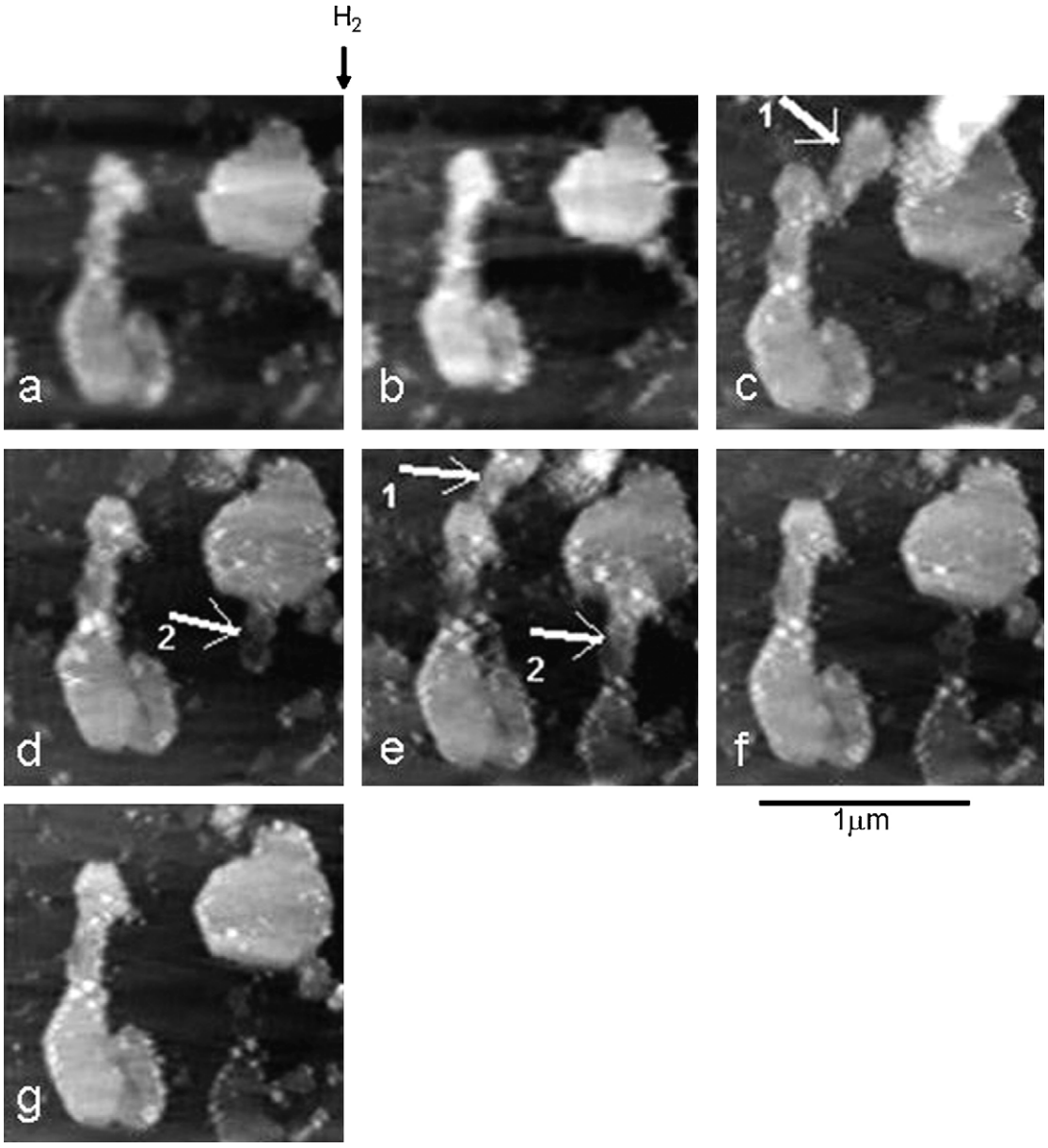

Fig. 3. STM images of a certain area on the sample, displayed in Fig. 1c (encircled), prior to (a) and following 1.5 L of H_2 exposure (b–g). The time interval between two consecutive images is about 30 min. The appearance and disappearance of some of the islands are marked by arrows. Imaging was performed with a bias voltage of 0.8 V and a current of 1.5 nA. The height span in the figures is ~16 nm.

ple was exposed to a dose of 1.6 L H_2, and specific hydride spots were imaged for a few hours. Then, an additional hydrogen exposure of 6.8 L H_2 was performed, followed by a few hours of imaging. Fig. 7 illustrates the time variations observed for specific hydride precipitates, during each of the above two stages. For the lower exposure, the hydride precipitates were relatively small (typical volumes of the order of 10^{-7} to 10^{-6} μm^3, an equivalent radius of a hemispherical shape being 20–50 Å). For the higher exposure the precipitates attained a larger size (typical volumes of the order of 10^{-5} to 10^{-4} μm^3, an equivalent radius of a hemispherical shape being 100–250 Å). However, in both cases, no regular growth of the hydride nuclei has been observed, but rather a fluctuating behavior, where random steps of either growth or shrinkage took place for each specific precipitate. Hence, it seems that for the above size scales, no spontaneous continuous growth is evident, even though it may be indicated (Fig. 7b) that the probability of shrinkage is lower for hydride precipitates larger than about 2×10^{-4} μm^3 (equivalent radius larger than 300–350 Å), where the extent of fluctuations seems to mitigate.

Besides the fluctuations in the size of the precipitates, also the shape of these nuclei has been altered with time. This is illustrated in Fig. 8, for a certain nucleus.

4. Discussion

4.1. Periodic appearance–disappearance of islands

In a recent publication [7], we have accounted for the phenomenon of "invisible" islands in the STM images, by the occurrence of an insulating layer between certain Gd islands and the W substrate. In such a case, the potential of the electrically floating island attains the potential of the tip and the STM current is controlled by the leak through the insulating interface layer. Hence, instead

Please cite this article in press as: H. Realpe, et al., J. Alloys Compd. (2008), doi:10.1016/j.jallcom.2008.06.013

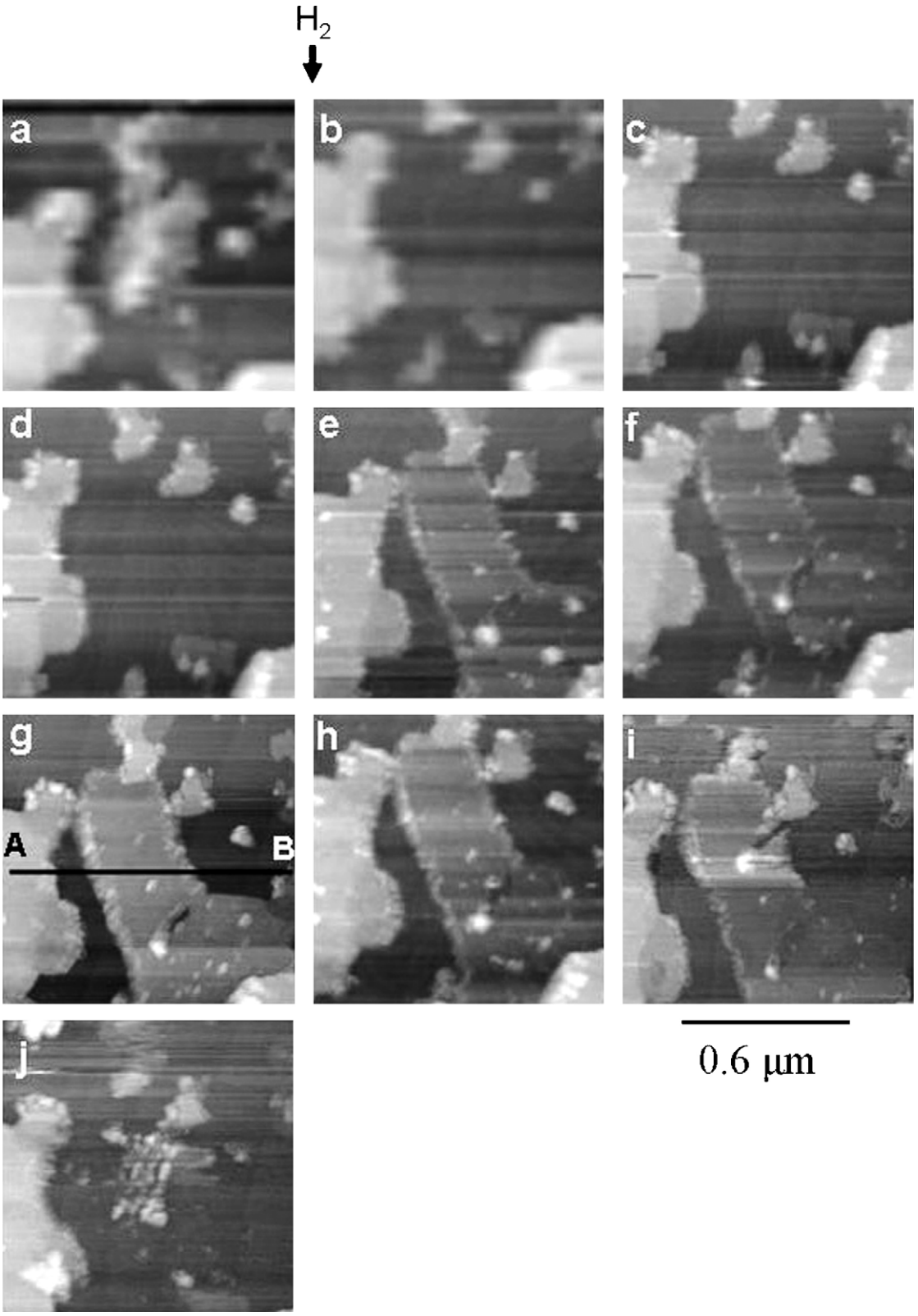

Fig. 4. STM images of another area on the sample displayed in Fig. 1c (marked by a rectangle), prior to (a) and following 1.5 L H_2 exposure (b–j). The time interval between images is about 30 min and imaging conditions are the same as for Fig. 3. The height span in the figures is ~16 nm. The line in (g) presents the height line scan illustrated in Fig. 5.

Please cite this article in press as: H. Realpe, et al., J. Alloys Compd. (2008), doi:10.1016/j.jallcom.2008.06.013

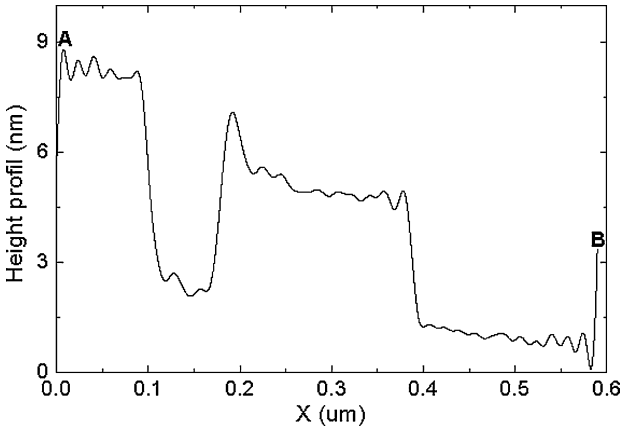

Fig. 5. Height profile across the line, marked in Fig. 4g.

of imaging the surface structure, the STM image reflects that of the Gd/W interface and the island is in fact transparent to the STM. In the present article, we shall focus on the role of hydrogen in the periodic appearance–disappearance of the Gd islands.

As described in Section 2.2.1, the Gd/W interface zone is rich in carbon and oxygen. The lateral distribution of these carbon/oxygen contaminations may vary, with some of the Gd islands being more isolated from the substrate than the others. Such islands may thus be transparent to the STM imaging process and be "invisible" before hydrogen exposure. It has been reported for some metal systems, evaporated on W(1 1 0) [10], that when the system metal/W(1 1 0) is exposed to hydrogen, hydrogen accumulates at the metal/W(1 1 0) interface. This accumulation may affect the conductivity properties of the carbon/oxide zone. Thus, for example [11], reactions of H with oxides may lead to partial oxide reduction, according to:

$$2H + 2O^{-2} \rightarrow 2OH^{-} + 2e^{-} \quad (1)$$

A well-known example of such a reversible hydrogen reaction is the reduction of WO_3 into $W_3O_3(OH)$ (i.e. the so-called "bronze"), where part of the W^{6+} ions in the oxide are reduced into W^{5+} valence [12], Such a reduction drastically changes the conduction properties of the oxide. Hence, dissolved hydrogen that reaches an isolating oxidized Gd/W boundary of an island may convert it into a more conductive interface, and the "invisible" island may become "visible".

The existence of such Gd islands with a conducting "switchable" interface, may thus serve as a probe for the local H concentrations at these interfaces. The periodic appearances and disappearances of these islands thus indicate local concentration fluctuations of the H atoms, dissolved in the specific island (forming the α-phase).

Unlike the conventional picture of averagely homogeneous, time independent, H concentration in the α-phase metal–hydrogen system, the above results point to inhomogeneous time fluctuating concentration gradients across the Gd(0 0 0 1)/W(1 1 0) sample. For a given island interface, periodic variations of the dissolved H concentration may occur with concentration build-ups and drops. As for concentration build-up, this process can take place, probably by diffusion of H atoms from neighboring islands or from the island's near surface region into the Gd/W interface, in a manner that will be explained below. Concentration drops, however, can take place by either one of two possible routs:

(i) Diffusion of H away from the island interface to its neighborhood (neighbor islands or the island's near surface region).
(ii) Nucleation of a hydride (β-phase) within the island. Since the concentration of H in the β-phase is much higher then in the α-phase such a hydride nucleus acts as a "pump" which diminishes the concentration of hydrogen around its surrounding.

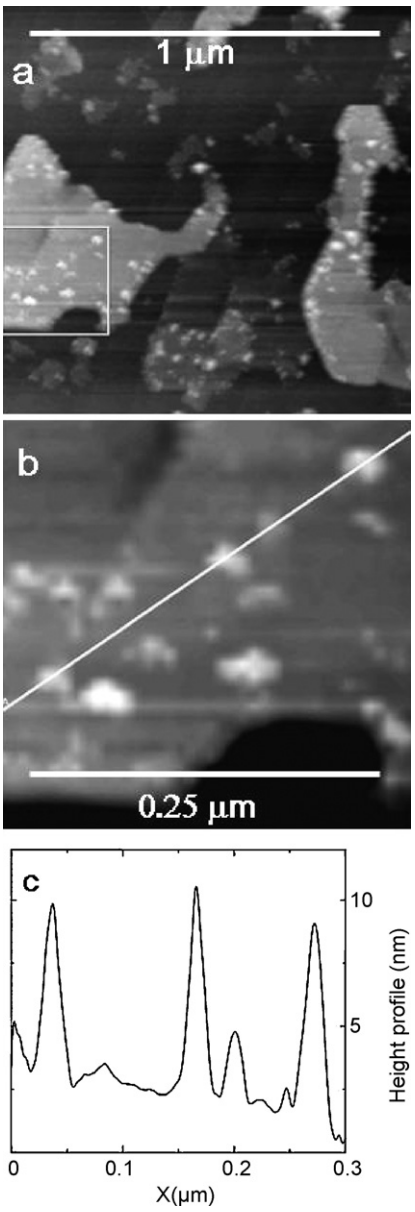

Fig. 6. Nucleation of the hydride (β-phase) on gadolinium islands: (a) hydride spots developed on an island (white spots in the marked rectangle); (b) enlargement of the above hydride spots; (c) height profile along the marked line in (b).

Observations of the periodic appearances–disappearances of different islands (such as those demonstrated in Figs. 3 and 4) point to the possible contributions of both above routs. In some cases, the disappearance of an island is concurrently accompanied by the appearance of hydride precipitates within the specific island. An example for such a case is given in Fig. 4j, where a cluster of hydride spots appeared at about the center of the vanishing island. In other cases, however, the disappearance of an island does not display clearly a concurrent hydride nucleation process. It seems then that "back-stream" diffusion causes the migration of H atoms from the island interface into its surrounding.

The question which may be addressed is: why should such "back-stream" diffusion take place? A possible answer to this question may be related to the mismatch strains at the Gd/W interface.

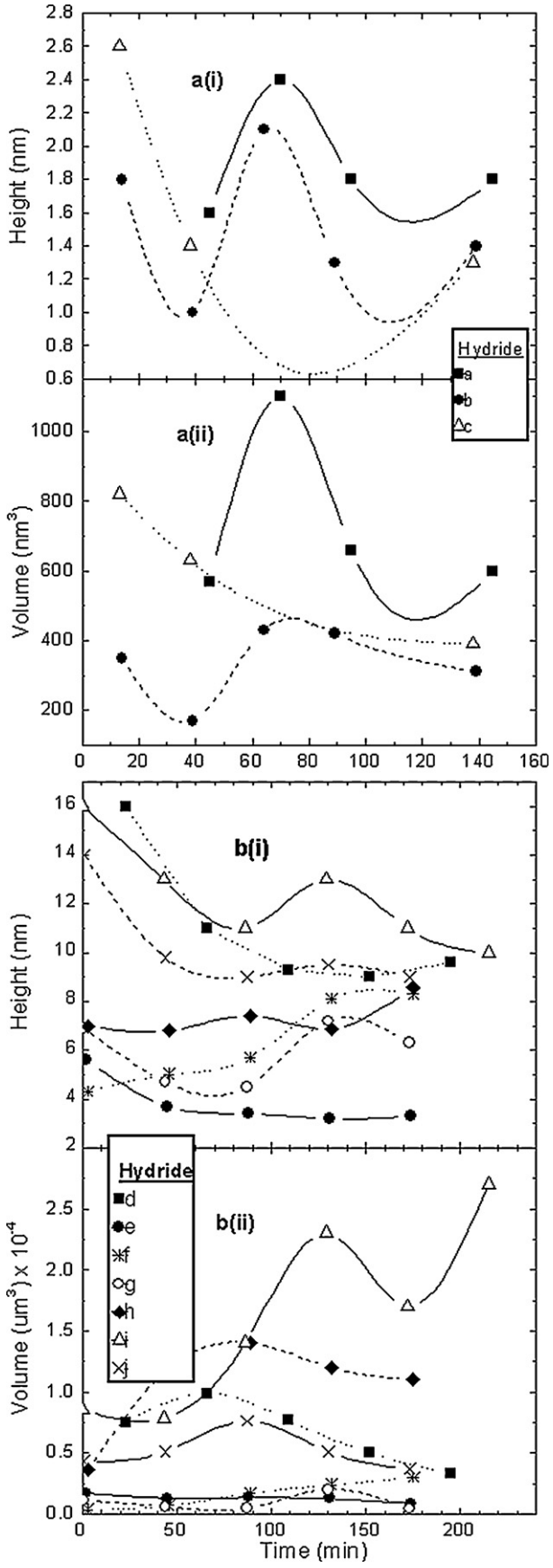

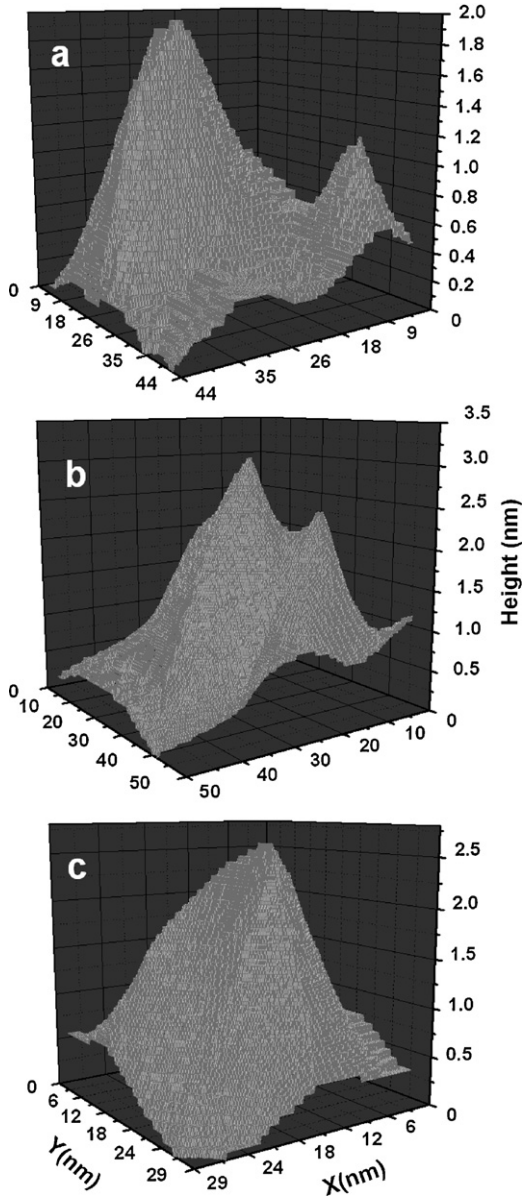

Fig. 8. The variations in the shape of a certain hydride precipitate, as a function of time (a–d). Time interval between consecutive images is about 30 min.

It has been reported [13,14], that the first monolayer of Gd on the W(1 1 0) surface possesses a strained hcp structure with a significant dilation (of about 8%, according to Ref. [13], or about 2% according to Ref. [14]). This misfit strain abruptly decreases with Gd thickness, and extends only to the second or third monolayer [13,14]. At these near-interface layers, however, the dilation in the Gd(0 0 0 1) planes can induce a contraction in the perpendicular interplanar spacing, leading to a reduction in the size of the interstitial sites, which occupy the dissolved H atoms. This will increase the energy of occupation of these sites and make them less favorable for H accommodation. Indeed, as reported by Getzlaff et al. [4,5], the adsorption of hydrogen in the first 2 or 3 ML of gadolinium is retarding relative to its adsorption on thicker islands.

Fig. 7. Size variations of hydride precipitates on Gd(0 0 0 1)/W(1 1 0) (similar to that displayed in Fig. 6b), as a function of time. Each line (and symbol) represents a specific precipitate. (a) After an exposure of 1.6 L H_2; (b) after an additional exposure of 6.8 L H_2. (i) and (ii) represent height and volume variations, respectively.

Please cite this article in press as: H. Realpe, et al., J. Alloys Compd. (2008), doi:10.1016/j.jallcom.2008.06.013

We can thus anticipate that the H dissolved in a particular Gd island will "stay away" from the near-interface region, due to the above misfit effect. Still, according to the proposed interpretation for the appearance of new islands, hydrogen atoms do reach the Gd/W interface region, reducing the oxidized interface layer. This controversy can be settled by assuming that the occurrence of the oxidized zone of the Gd/W interface provides a gradual misfit region and diminishes the abrupt misfit gradient between the first Gd layer and the next W layer, enabling the H atoms reaching this zone and reducing it according to Eq. (1). At this stage the island appears. At a certain extent of reduction, however, the oxidation zone is not providing the gradual misfit gradient anymore and the abrupt misfit strain between the Gd and W layers starts to prevail, driving away the local H atoms and starting the reverse branch of Eq. (1), i.e. reoxidation, leading to re-disappearance of the island. It has to be noted that other cyclic surface reactions, in which the reaction product destabilizes the equilibrium, causing a reversal and vice versa had been reported before, by the Ertle group [15].

4.2. Hydride nucleation and growth

It should be emphasized that the present behavior of hydride nucleation and growth on the Gd islands is associated with a fixed (small) amount of hydrogen, retained in the system (following a certain H_2 exposure and pumping), and not with the usual case, in which a certain metallic system is continuously exposed to hydrogen.

As described in Section 3.2, the size and shape of the formed hydride precipitates change randomly and certain nuclei display intermittently growth and shrinkage steps (Figs. 7 and 8). There are two possibilities to account for such a fluctuating behavior:

(i) The sizes of the precipitates are below their nucleation critical values, i.e. are rather embryos than nuclei.
(ii) The fluctuations are associated with corresponding H concentration fluctuations in the α-phase, surrounding a certain hydride precipitate.

The critical size, r_c, of a solid state nucleus is given by Ref. [16]:

$$r_c \cong \frac{2\sigma}{\Delta E_v} \quad (2)$$

with σ the nucleus–matrix interface energy per unit area and ΔE_v the free energy gain of the nucleus formation per unit volume.

For a hydride nucleus, the bulk free energy term may be approximated by

$$\Delta E_v \cong \frac{\Delta G_{f\rho_h}}{M_h - \Delta E_s} \quad (3)$$

with ρ_h the weight density of the hydride, M_h the molecular weight, ΔG_f the free energy of formation of the hydride per mole H_2 and ΔE_s the elastic strain energy per unit volume associated with the expansion of the nucleus in the metal matrix. For GdH_2 [17] $\Delta G_f \approx 37.7$ kcal/(mole H_2), $\rho_h = 7.1$ g/cm^3, $M_h = 159.2$, which yields a bulk chemical energy term of about 1700 cal/cm^3. The elastic energy term, ΔE_s, has recently been established for the GdH_2/Gd system [18], to be about 40 cal/cm^3, i.e. only about 2% of the bulk free energy term, hence may be neglected in this case. Finally, the interface energy, σ, even though not known for this system, can be approximated by a certain upper limit typical to solid–solid interfaces, of about 10^{-5} cal/cm^2 [0.4 J/cm^2]. Substituting these values into Eqs. (3) and (2), one gets $r_c \approx 1$–2 Å, i.e. a critical size of nucleus composed of a few atoms only. This size is about two orders of magnitude smaller than the size scale of the hydride precipitates displayed in Fig. 7. Hence, it is unlikely that possibility (i) (i.e. sub-critical size) can account for the fluctuating behavior of those hydride precipitates.

It seems thus, that hydrogen concentration "waves" occur within the gadolinium α-phase islands, causing the non-regular growth–shrinkage phenomenon of the hydride precipitates. However, unlike the case of the oxidized Gd/W interface, discussed previously, where a possible mechanism, inducing such fluctuating behavior, can be proposed (i.e. the reversible reduction–oxidation of the interface oxide, Eq. (1)), it is not evident to conceive such a mechanism for the present case. A possible explanation can be associated with the increased elastic strain induced by the hydride growth. This strain field which increases the energy of the occupied H sites may lead to a back-stream diffusion of hydrogen from the hydride–metal interface, reducing the local near-interface H concentration below the solubility limit, followed by dissolution (shrinkage) of the hydride precipitate. The shrinkage of the hydride precipitate then relaxes the strain field at the surrounding α-phase matrix, which in turn "pumps" again hydrogen, inducing the hydride to grow again.

Such a period mechanism may probably account for the observed size and shape fluctuations of the formed precipitates.

5. Conclusions

1. STM observations of hydrogen exposed Gd(0 0 0 1) islands grown on a W(1 1 0) substrate, indicate that the H concentrations within the α-phase Gd islands are not homogeneously distributed, but rather fluctuating, forming "waves" of high and low concentrations intermittently.
2. Under certain conditions, the Gd islands may become transparent to the STM, "disappearing" from the STM image. Such conditions are attained when the island is electrically insulated from the substrate due to the existence of a certain insulating interface layer (e.g. oxide).
3. A possible mechanism inducing fluctuating H concentration "waves" in the α-phase is proposed. It is associated with the reversible reduction–oxidation of the Gd/W interface oxide (which induces periodic appearance–disappearance of the respective Gd islands).
4. The precipitation of the hydride (β-phase) within the α-phase, also displays an irregular growth behavior, with randomly alternating growth–shrinkage steps concurrent with random shape changes of the developing nuclei.
5. The above irregular development of the hydride may be due to the elastic strain field associated with the hydride nuclei growth within the α-phase matrix.

Acknowledgements

This work was partially supported by a grant from the Israel Council for Higher Education and the Israel Atomic Energy Commission and a grant from the Ministry of National Infrastructure, Division of R&D.

References

[1] R. Arkush, A. Venkert, M. Aizenshtein, S. Zalkind, D. Moreno, M. Brill, M.H. Mintz, N. Shamir, J. Alloy Compd. 244 (1996) 197.
[2] Y. Ben-Eliyahu, M. Brill, M.H. Mintz, J. Chem. Phys. 111 (1999) 6053.
[3] M.H. Mintz, in: K.H.J. Buschow, R.W. Cahn, M.C. Flemings, B. Ilschner, E.J. Kramer, S. Mahajan (Eds.), Encyclopedia of Materials: Science and Technology, Elsevier Science, 2002, pp. 1–9.
[4] M. Getzlaff, M. Bode, R. Wiesendanger, Surf. Sci. 410 (1998) 189.
[5] M. Getzlaff, M. Bode, R. Pascal, R. Wiesendanger, Phys. Rev. B 59 (1999) 8195.
[6] A. Pundt, M. Getzlaff, M. Bode, R. Kirchheim, R. Wiesendanger, Phys. Rev. 61B (2000) 9964.

[7] H. Realpe, N. Shamir, M.H. Mintz, Y. Manassen, Surf. Sci. 600 (2006) 2795.
[8] A. Aspelmeier, F. Gerhardter, K. Baberschke, J. Magn. Magn. Mater. 132 (1994) 22.
[9] E.D. Tober, R.X. Ynzunza, C. Westphal, C.S. Fadley, Phys. Rev. B 53 (1996) 5444.
[10] J.E. Whitten, R. Gomer, Surf. Sci. 316 (1994) 23.
[11] T. Seiyama, in: J. Nowotny, L.-C. Dufour (Eds.), Surface and Near-Surface Chemistry of Oxide Materials, Elsevier Science Publisher B.V., Amsterdam, 1988, pp. 189–217.
[12] G.L. Frey, A. Rothschild, J. Sloan, R. Rosenstveig, R. Popovitz-Biro, R. Tenne, J. Solid State Chem. 162 (2001) 300;
J. Sloan, J.L. Hutchison, R. Tenne, Y. Feldman, T. Tsirlina, M. Homyonfer, J. Solid State Chem. 144 (1999) 100 (and references therein).
[13] D. Weller, S.F. Alvarado, J. Appl. Phys. 59 (1986) 2908.
[14] S.A. Nepijko, M. Getzlaff, R. Pascal, Ch. Zarnitz, M. Bode, R. Wiesendanger, Surf. Sci. 466 (2000) 89.
[15] R. Imbihl, M.P. Cox, G. Ertl, H. Muller, W. Brenig, J. Chem. Phys. 83 (1985) 1578.
[16] J.W. Christian, The Theory of Transformations in Metals and Alloys. Part I. Equilibrium and General Kinetic Theory, second ed., Pergamon, New York, 1975.
[17] W.M. Mueller, J.P. Blackledge, G.G. Libowitz, Metal Hydrides, Academic Press, New York, London, 1968, Chapter 9.
[18] Y. Greenbaum, D. Barlam, M.H. Mintz, R.Z. Shneck, J. Alloy Compd. 452 (2008) 325.

Please cite this article in press as: H. Realpe, et al., J. Alloys Compd. (2008), doi:10.1016/j.jallcom.2008.06.013